J. Fluid Mech. (1978), *vol.* 89, *part* 3, *pp.* 515–533
Printed in Great Britain

Coherent structures in the outer mixing region of annular jets

By W. T. CHAN AND N. W. M. KO

Department of Mechanical Engineering,
University of Hong Kong

(Received 24 February 1978)

This paper describes in detail the overall pressure and spectral results in the outer mixing region of three annular jets. The outer mixing region can be considered as the result of the shearing of a single jet by the ambient air. The coherent structures found consist of an array of toroidal jet vortices convecting downstream in the outer mixing region. The structures tend to agree with the ones for a single jet.

1. Introduction

The annular jet has been incorporated into the basic design of burning and fluidic devices (Chigier & Beer 1964; Davies & Beer 1969; Beer & Chigier 1972; Vanderbury 1973; and others). Owing to these applications, a basic understanding of the aerodynamic process and flow structures is important and necessary.

Annular jet flow was studied as a limiting case of a coaxial jet by Chigier & Beer (1964) and Williams, Ali & Anderson (1969). The stabilizing effect of an annular jet in a flame jet was also studied by Chigier & Beer (1964) and Davies & Beer (1969). However, because of the inherent complexity of the flow structures within the annular jet, basic understanding of the structures, especially in the initial region, was limited.

A better understanding of the fundamental characteristics of a single jet, as reported by Davies, Fisher & Barratt (1963), Bradshaw, Ferriss & Johnson (1964), Fisher & Davies (1964), Crow & Champagne (1971), Lau, Fisher & Fuchs (1972) and others, should be extremely useful in the basic understanding of the much more complicated structure of annular jets. Thus in the present investigation of annular jets, knowledge about the single jet was heavily relied upon and used.

Part of the results of the present investigation have already been reported (Ko & Chan 1978). These results mainly concerned the mean velocity, turbulence intensity and the similarities of the profiles of three annular jets: a basic annular jet, a conical jet and an ellipsoidal jet. This paper presents the pressure fluctuations and the spectra which are associated with the jet vortices in the outer mixing region. The pressure fluctuations and spectra associated with the wake vortices will be presented in another paper and hence will be only briefly discussed here.

The choice of the three annular jets is important and necessary for the isolation of the contributions from these different vortices. In addition, a simple model of the structures in the initial region is proposed. This very simple model allows comparison with the better known structure of single jets.

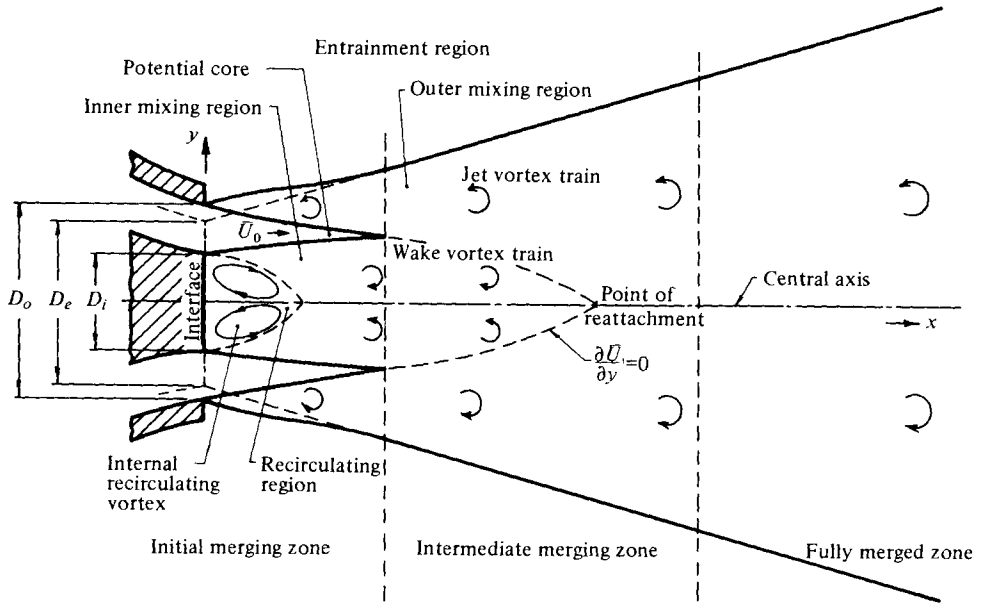

FIGURE 1. Schematic diagram of basic annular jet.

2. The model of flow structures

In earlier work, Ko & Chan (1978) have separated annular jets into the initial merging, intermediate merging and fully merged zone. Within these three zones, similarity of the mean velocity and turbulence intensity profiles has been observed.

The initial merging zone extends from the jet exit plane to the tip of the potential core (see figure 1). In the intermediate merging zone, the basic annular jet reattaches at the central axis, i.e. the line $\partial \bar{U}/\partial y = 0$ intersects the central axis. Slightly further downstream of the point of reattachment, the jet is fully developed and the fully merged zone begins.

Within these different zones a simple model is proposed to explain the basic flow structures. The basic structures are summarized in the following sections.

In the initial merging zone, the outer mixing region of an annular jet, be it of the basic annular, conical or ellipsoidal type, is the result of the shearing of a single jet of diameter D_o and mean exit velocity $\bar{U}_0$ by the ambient fluid. Thus, as in the case of a single jet, this mixing region of the annular jet is occupied by a toroidal vortex street which is similar to that of a single jet (figure 1). According to the results for a single jet, these vortices convect downstream with a velocity of $\sim 0{\cdot}6\,\bar{U}_0$. The axial separation between these successive jet vortices is $\sim 1{\cdot}25 D_o$. The corresponding Strouhal number $f_j D_o/\bar{U}_0$ of the spectral peak is about 0·6.

In the intermediate merging zone vigorous mixing of the flow inherited from the mixing region upstream occurs. A new mixing region is thus generated, resulting in a new spreading rate. It is also within this zone that the mixing of the two types of vortices, the jet vortices from the outer mixing region and the wake vortices from the internal recirculating region, occurs. The Strouhal number $f_w D_i/\bar{U}_0$ of the wake

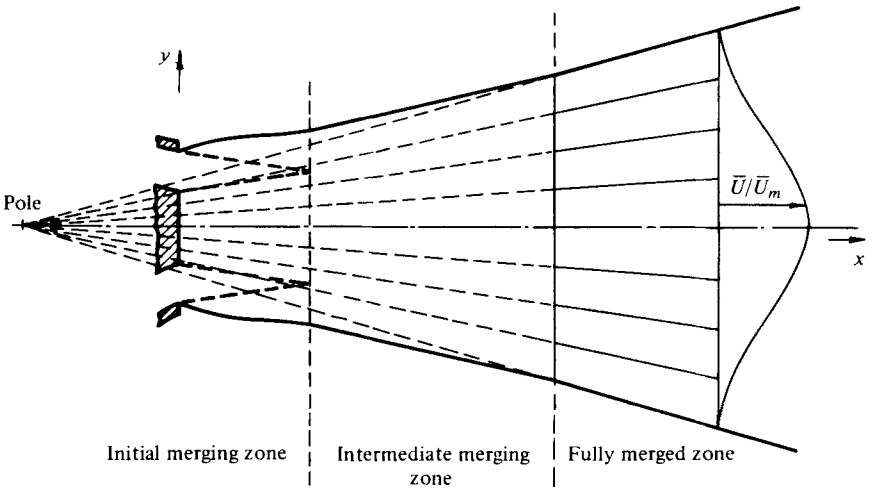

FIGURE 2. Schematic diagram of fully merged zone of annular jet.

vortices is $\sim 0{\cdot}3$. This means that in this intermediate merging zone the jet vortices from the outer mixing region are preferred and grow.

The mixing of the flow is almost complete at the axial position where the basic annular jet reattaches to the central axis. An additional distance downstream of $1\text{–}1{\cdot}5D_o$ is required for the flow to become fully developed. For the ellipsoidal and conical jet fully developed flow occurs at about five diameters downstream of the nozzle exit.

In the fully merged zone the annular jet, be it basic, ellipsoidal or conical, behaves like the main region of a single jet (figure 2). The maximum mean velocity occurs at the central axis. The curves $\bar{U}/\bar{U}_m$ = constant in this zone are straight lines and converge to a point which is referred as the virtual origin or pole. The axial position of the pole is found to be upstream of the nozzle exit. Further, the maximum mean velocity at each axial plane is inversely proportional to the axial distance from the pole (Abramovich 1963, p. 15).

3. Apparatus

The experimental rig employed has been described by Ko & Chan (1978). The basic annular jet has an outer diameter D_o of 6·2 cm and an inner diameter D_i of 2·8 cm at the nozzle exit. This basic annular jet has an internal recirculating vortex of toroidal form (Chigier & Beer 1964). The other two types of annular jets, conical and ellipsoidal, contain a bullet-like protrusion whose purpose is to eliminate the internal recirculating vortex. The length of both the conical and the ellipsoidal bullet was $1{\cdot}5D_o$. In this respect, the effect and interference of the internal recirculating vortex was eliminated from the results.

The hot-wire anemometry used has been described elsewhere (Ko & Chan 1978). A tungsten wire of diameter 5×10^{-6} m with a sensing length of 2 mm was used for the velocity measurements. The pressure measurements were obtained by using a standard Brüel & Kjaer $\frac{1}{8}$ in. condenser microphone with the proper nose cone.

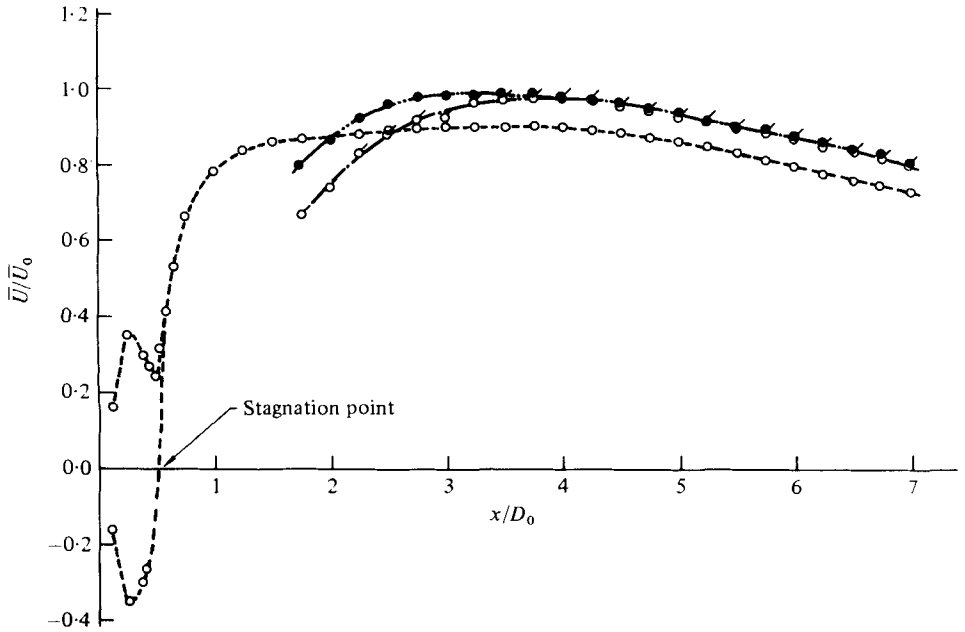

FIGURE 3. Mean velocity distributions along the central axis of the three annular jets ($y/D_0 = 0$). ○, basic annular jet; ●, conical jet; ♂, ellipsoidal jet.

The analysing equipment consisted of a Brüel & Kjaer frequency analyser Type 2107 and a Brüel & Kjaer level recorder Type 2307; 6 % bandwidth filters were used for the spectral analysis.

The domain of investigation was mostly confined to the first five outer diameters D_0 downstream of the nozzle exit. Further, the main effort was expended on the outer mixing region, where the jet vortices were present. The mean exit velocity in the investigation was 50 m/s.

4. Mean velocity

Since the earlier work has reported the radial distributions of the mean axial velocity in the three zones, this section concerns only the axial distribution of the mean velocity at the central axis $y/D_0 = 0$ of the three annular jets.

The axial distribution of the mean velocity of the basic annular jet shows a small peak of $0{\cdot}35\bar{U}_0$ at $x/D_0 = 0{\cdot}25$ (figure 3). Beyond the axial position $x/D_0 = 0{\cdot}5$ the mean velocity increases fairly rapidly initially and then much more gradually to a maximum of about $0{\cdot}91\bar{U}_0$. Because of the occurrence of backflow close to the interface at the nozzle exit and the inability of the hot wire to determine the flow direction, the small peak at $x/D_0 = 0{\cdot}25$ can be interpreted as that due to the reverse flow (Miller & Comings 1960; Chigier & Beer 1964; Carmody 1964; Davies & Beer 1969). The stagnation point which marks the end of the recirculating region cannot be determined directly from the measurements. This is due to the poor resolution of the hot wire and the fluctuating flow around this point. Instead, the sign of the velocity of the small peak at $x/D_0 = 0{\cdot}25$ is arbitrarily reversed. The flow near the stagnation

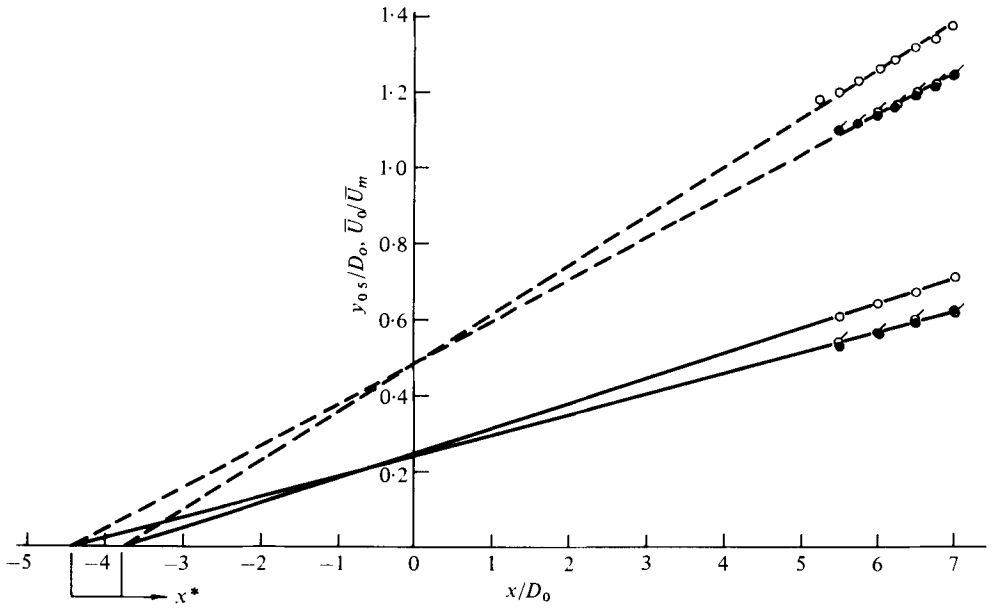

FIGURE 4. Positions of the poles of the fully merged zones of the three annular jets. ——, $y_{0.5}/D_o$; – – –, $\bar{U}_0/\bar{U}_m$. Other symbols same as in figure 3.

point is corrected by extrapolation from the less turbulent flow field downstream, as shown by the dashed curves in figure 3. The stagnation point is thus estimated to be at $x/D_o = 0{\cdot}5$ ($x/D_i = 1{\cdot}10$). In other words, the recirculating region extends to $x/D_o \simeq 0{\cdot}5$.

The axial distributions of the mean velocity of the conical and ellipsoidal jet are also shown in figure 3. A difference between the mean velocities of these two jets is found for $x/D_0 \leqslant 4$, with that of the conical jet higher than that of the ellipsoidal jet. The higher velocity is mainly due to the loss in the smaller wake formed behind the tip of the conical bullet being lower than that for the ellipsoidal bullet. This difference in the losses can also be seen by comparing the mean velocities of the conical and ellipsoidal jets with that of the basic annular jet at axial positions $x/D_o \geqslant 4$. The absence of the bullet in the centre of the basic annular jet results in a reduction of $\bar{U}/\bar{U}_0 = 0{\cdot}08$.

In the fully merged zone the similarity of the mean velocity profiles, as observed by Ko & Chan (1978), suggests a virtual origin or pole of the three annular jets. The location of the pole, based on the radial position $y_{0.5}$ corresponding to $\bar{U}/\bar{U}_m = 0{\cdot}5$, is shown in figure 4. There is a slight difference in the positions for the basic annular jet and the conical and ellipsoidal jets, the axial position being $-3{\cdot}8D_o$ for the former and $-4{\cdot}4D_o$ for the latter two. The agreement between the latter two annular jets shows that the shape of the bullet does not really affect the flow in this fully merged zone.

These positions of the virtual origin or pole may also be found from the axial distributions of the mean velocity at the central axis (figure 3). The results are replotted in the form $\bar{U}_o/\bar{U}_m$ in figure 4, which illustrates very clearly that the mean velocity is inversely proportional to the axial distance x^* from the pole. This relationship is found for all three annular jets considered.

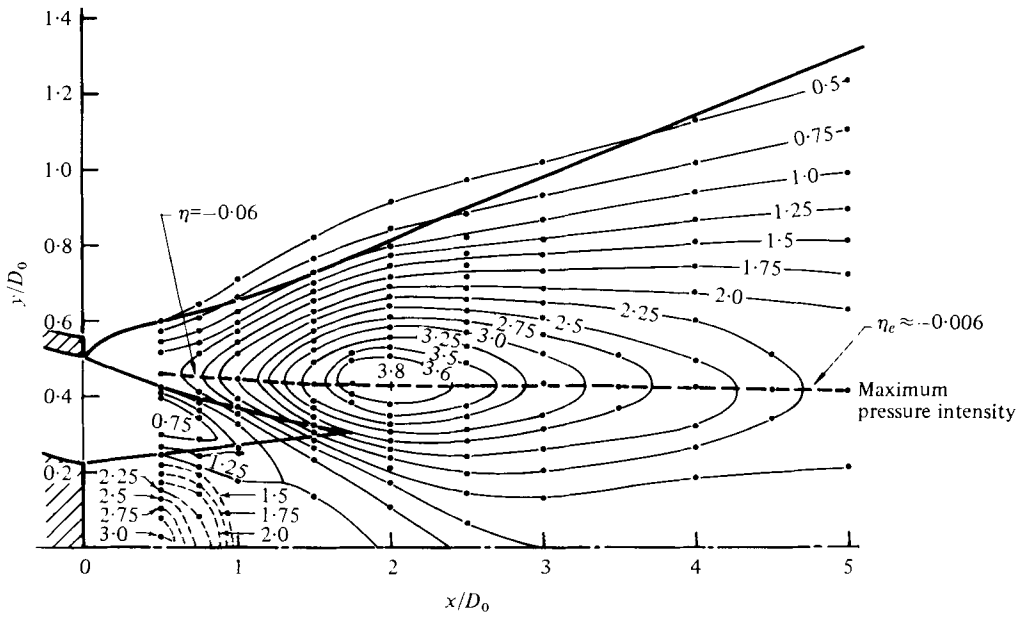

FIGURE 5. Contours of overall pressure intensity of basic annular jet. (The numbers labelling the curves are $\tilde{p}/\rho_0 \bar{U}_0^2$ expressed as a percentage.)

On the basis of the spread of the $\bar{U}/\bar{U}_m = 0{\cdot}5$ contours, the tangent of the spreading angle for the basic annular jet is 0·066 rad, while that for the conical and ellipsoidal jets is 0·054 rad, which is smaller by about 0·7°. The corresponding result for a single jet is 0·097 rad. This means that the spread of the basic annular jet is smaller than that of the single jet by 1·8° while that of the conical and ellipsoidal jets is smaller by 2·5°.

5. Overall pressure intensity

The distributions of the overall r.m.s. pressure intensity $\tilde{p}/\rho_0 \bar{U}_0^2$ of the basic annular jet and the ellipsoidal jet are shown in figures 5 and 6. The actual data points are shown as circles in the figures. Since the data points for the conical jet are basically the same as those for the ellipsoidal jet they are not presented here (Chan 1977). In the initial region of the basic annular jet two peaks are found in the pressure distributions (figure 5). As will be discussed in another paper, the peak at and very near the interface is due to the internal recirculating or wake vortex. The other peak is found inside the outer mixing region. The maximum pressure intensity of this peak is found near the axial position $x/D_o = 2$ and has an overall intensity of $\tilde{p}/\rho_0 \bar{U}_0^2 = 3{\cdot}8\,\%$. Also shown in figure 5 is the locus of the maximum pressure intensity. The locations of these maxima are found within $0{\cdot}40 < y/D_o < 0{\cdot}45$. There is a tendency for the locus to shift towards the central axis.

In the ellipsoidal jet the absence of the internal recirculating vortex at the central axis is responsible for the disappearance of the peak in that region (figure 6). However, the peak inside the outer mixing region is still present. The maximum pressure intensity of this peak is found further downstream, at $x/D_o = 3{\cdot}5$, and has an overall intensity of

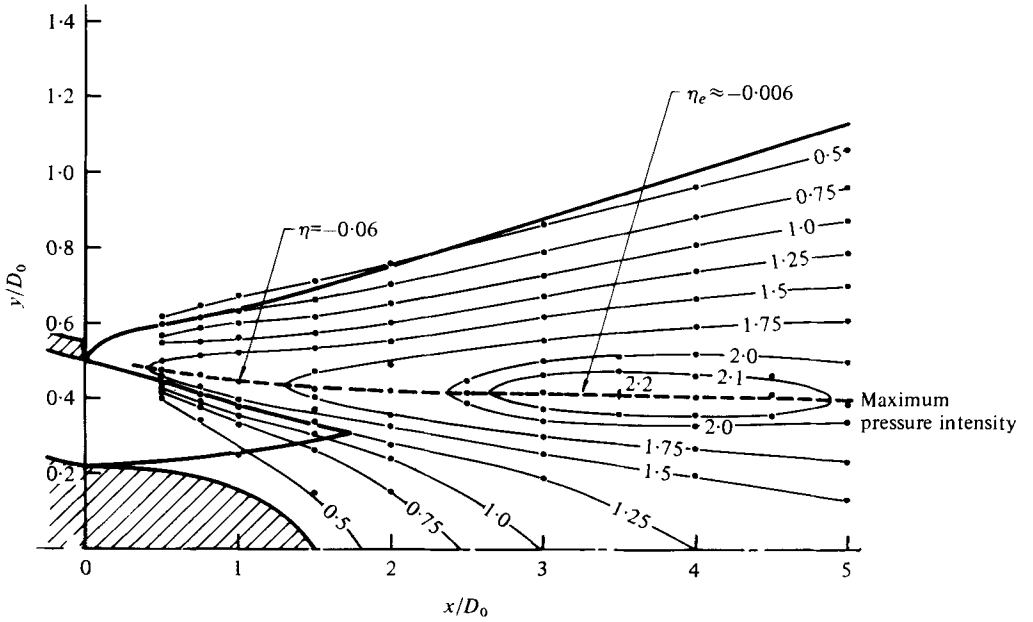

FIGURE 6. Contours of overall pressure intensity of ellipsoidal jet.

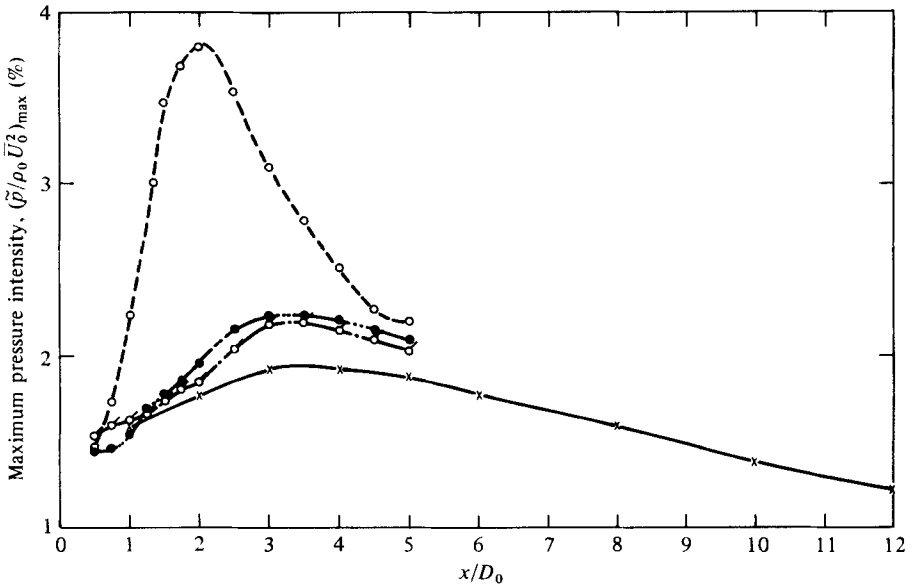

FIGURE 7. Axial distributions of the maximum overall pressure intensity of the three annular jets. ×, single jet ($D = 2$ cm, $\bar{U}_0 = 50$ m/s). Other symbols same as in figure 3.

$\tilde{p}/\rho_0 \bar{U}_0^2 = 2{\cdot}2\,\%$. The locations of the maximum pressure intensity tend to be slightly displaced towards the central axis. The displacement is slightly more for $x/D_o \leqslant 2$ and less for $x/D_o > 2$.

Comparison of figures 5 and 6 indicates that the difference in the overall pressure intensity is due to the presence of the central ellipsoidal bullet. In the basic annular

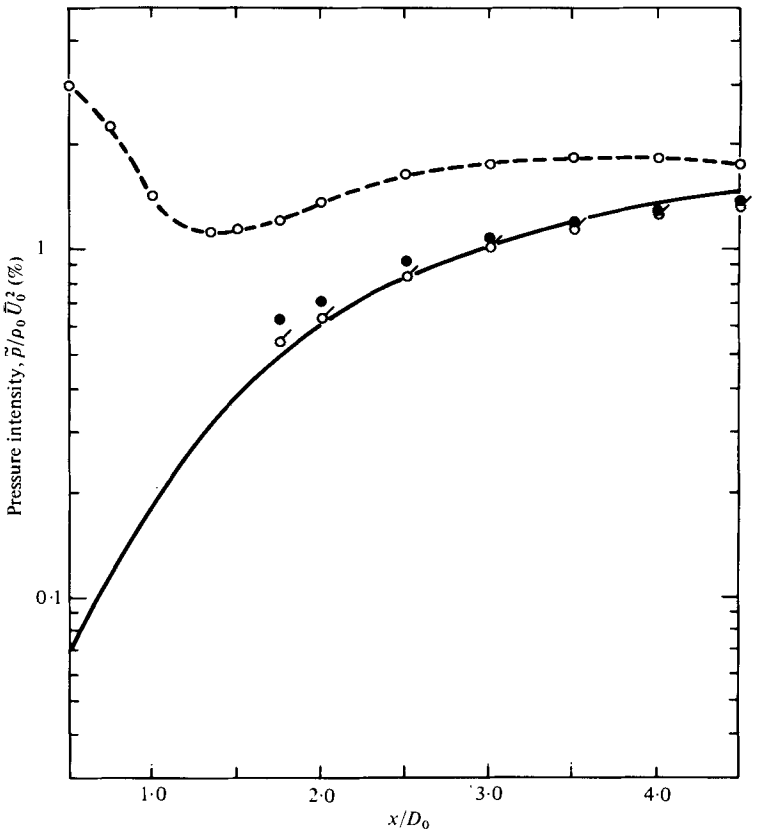

FIGURE 8. Overall pressure intensity along central axis of the three annular jets ($y/D_0 = 0$). ——, Fuchs (1972). Other symbols same as in figure 3.

jet the presence of the internal recirculating vortex is responsible for the higher pressure intensity (by 1·6 %) in the outer mixing region. In addition, because of the internal recirculating region the peak pressure intensity of the basic annular jet is found at around $x/D_o = 2$ instead of at $x/D_o = 3{\cdot}5$ as for the ellipsoidal jet. Furthermore, the contours of the pressure intensity are not as elongated as those for the ellipsoidal jet. Although the pressure intensity of the basic annular jet is much higher, the more rapid decrease in the intensity in the radial direction means that the contour $\tilde{p}/\rho_0 \bar{U}_0^2 = 0{\cdot}5\,\%$ falls roughly on the jet's outer boundary (figure 5). This phenomenon is also observed in the ellipsoidal jet (figure 6). This leads to the interesting fact that, although the geometry at the interface affects the pressure intensity distribution inside the jet, the intensity at the outer boundary is more or less independent of the conditions inside. This has also been observed in the turbulence intensity distributions reported by Ko & Chan (1978).

A more detailed comparison of the maximum pressure intensities of the three annular jets is shown in figure 7. The results for a 2 cm single jet with $\bar{U}_0 = 50$ m/s are also included in the figure. The difference between the results for the conical and ellipsoidal jets is marginal, with the former slightly higher than the latter. However, there is a slight tendency for the peak of the former to shift closer to the

nozzle exit. Compared with a single jet, the intensities of the conical and ellipsoidal jets are slightly higher and the peaks slightly nearer the nozzle exit. Nevertheless, in the fully merged zone ($x/D_o > 5$) there is a tendency for the results for these two annular jets to approach those for a single jet.

The maximum pressure intensity of the basic annular jet is not only much higher than those of the other two annular jets but also the peak location is much more prominent (figure 7). As for the other two annular jets, in the fully merged zone the intensity of the basic annular jet approaches the single-jet results.

The pressure intensity along the central axis ($y/D_o = 0$) of the three annular jets is shown in figure 8. The results for a single jet of Fuchs (1972) are also included for comparison. It is very interesting to find that the intensities of the conical and ellipsoidal jets agree very well with those of the single jet. For the basic annular jet, however, the high pressure intensity very near the nozzle exit, $x/D_o \leqslant 1{\cdot}35$, is due to the internal recirculating or wake vortex. The effect of the shedding of the wake vortices is still felt up to $4{\cdot}5D_o$ downstream. Even though the effect of the wake vortices is felt after $x/D_o > 1{\cdot}35$, the contribution of the jet vortices to the overall pressure intensity on the central axis becomes obvious. This may be the reason for the increase in the pressure intensity of the basic annular jet at the central axis and for the peak observed at $x/D_0 \simeq 3$ (figure 8).

The pressure intensity peak at the central axis of the basic annular jet is about one outer diameter D_o further downstream than that at the maximum intensity (figure 7). The reason for this difference in position may be the combined effect of the directivity, the tendency of the jet vortices to move towards the axis and the rapid deterioration of the shed wake vortices during their propagation downstream.

Kwan & Ko (1977) have suggested that the locations of the peak pressure intensity in the mixing region of a single jet and coaxial jets indicate the possible locations of the vortices. They found that the jet vortices of the coaxial jets lie along $\eta = -0{\cdot}06$, where the non-dimensional radial distance η was individually scaled for the primary and secondary jet vortices. Lau (1971) and Ko & Davies (1975) have also suggested that within the mixing region the vortex path in a single jet is close to

$$\eta = (y - \tfrac{1}{2}D)/x = -0{\cdot}06.$$

For the present investigation the locations of the peak pressure intensity are also shown in figure 5 and 6. Within a distance $1{\cdot}25D_o$ downstream of the nozzle exit the locations of the maximum pressure intensity of both the basic annular and the ellipsoidal jet lie along $\eta = (y - \frac{1}{2}D_o)/x = -0{\cdot}06$. This agreement of the peak locations within the axial distance $x/D_o \leqslant 1{\cdot}25$, i.e. within the initial merging zone, suggests that the internal subatmospheric region does not really affect the location of the jet vortices found in the outer mixing region.

In addition, the above annular-jet results agree very well with the results for a single jet and coaxial jets. This agreement within $x/D_o \leqslant 1{\cdot}25$ may further suggest that the jet vortices are not so easily affected during their formation and during their initial propagation downstream.

For axial positions $x/D_o > 1{\cdot}25$ the locations of the peak pressure intensity change and their loci become more parallel to the central axis (figure 5 and 6). Detailed comparison between the results for the three annular jets shows that the locations are roughly the same: $\eta_e = (y - \frac{1}{2}D_o)/x \approx -0{\cdot}006$. This change in the path of the jet

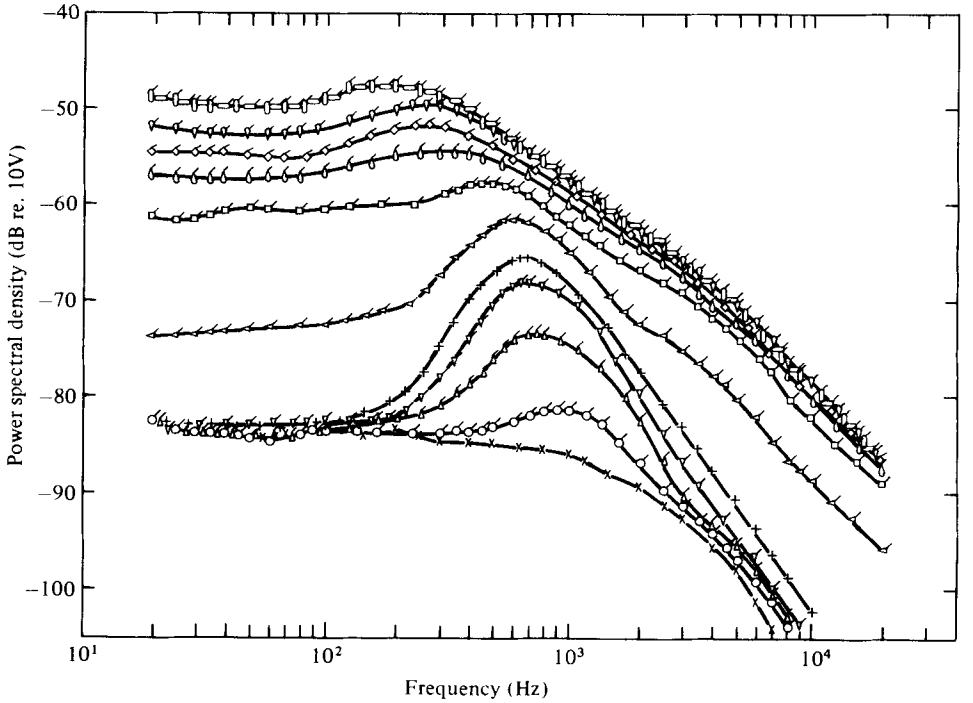

FIGURE 9. Spectra of hot-wire signals for ellipsoidal jet ($y/D_0 = 0{\cdot}3$). x/D_0: ×, 0·25; ○, 0·5; △, 0·75; ▽, 1; +, 1·25; ◁, 1·5; Y, 1·75; □, 2; ⬡, 2·5; ◇, 3; ⬠, 3·5; ⬡, 4; ⬭, 4·5.

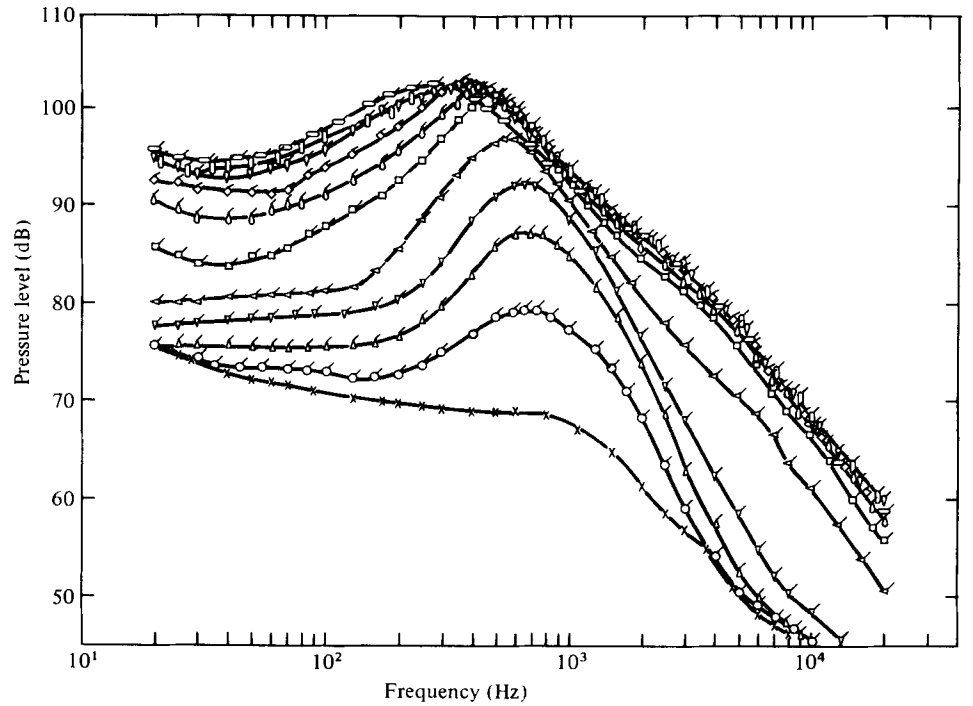

FIGURE 10. Spectra of microphone signals for ellipsoidal jet ($y/D_0 = 0{\cdot}3$). Symbols same as in figure 9.

vortices in the intermediate and fully merged zone to a path more parallel to the central axis may be due to interaction of the jet vortices coming from the initial merging zone.

This change in the direction of propagation of the jet vortices has been found in the secondary vortices of coaxial jets (Kwan & Ko 1977). According to these workers, the axial position at which the change in direction occurs is near the end of the secondary potential core. Thus this agrees with the results of the present investigation.

The above discussion on the path of the jet vortices in the intermediate and fully merged zone should be treated with reservation. The main reason is the fairly flat pressure intensity distribution. The flatness of the distribution makes the precise determination of the change from $\eta = -0{\cdot}06$ in the initial merging zone to $\eta_e \approx -0{\cdot}006$ in the intermediate merging and fully merged zone very difficult.

6. Spectrum inside annular jets

A spectral analysis of both the velocity and the pressure fluctuations inside the three annular jets has been performed. A set of the spectra of the fluctuations along $y/D_o = 0{\cdot}3$ for the ellipsoidal jet is shown in figures 9 and 10. The effect of the background turbulence on the hot-wire signals can be easily seen in figure 9. This means that the high turbulence intensity for $x/D_o \geqslant 2$ makes it more difficult to interpret the contribution of the jet vortices. For this reason the pressure spectra are presented because of the slightly better emergence of the jet vortices from the background turbulence (Ko & Kwan 1976). Even with the above reservation, both figures indicate the presence of the spectral peak, which is found within the axial region

$$0{\cdot}5 \leqslant x/D_o \leqslant 2{\cdot}5.$$

In the initial merging zone the radial position $y/D_o = 0{\cdot}3$ is very near the axis of the potential core (figures 5 and 6). This means that the spectra may be compared with the ones obtained on the axis of a single jet (Ko & Davies 1971). It is observed that the spectra of the velocity fluctuations near the axis of the potential core of the ellipsoidal jet (figure 9) are very similar to those of the single jet. The building-up of the broad peak from very near the nozzle exit ($x/D_o = 0{\cdot}25$) to the end of the potential core is common to the ellipsoidal annular and single jet. Furthermore, the shapes and sizes of the broad spectral peaks of these two types of jet are also very similar. This good similarity only points to the fact that, as in the case of a single jet, the broad peak observed in the ellipsoidal jet is due to the jet vortices present in the outer mixing region.

The above argument can be further supported by the findings presented in § 5 on the overall pressure intensity, as illustrated in figure 8. As has been shown by Ko & Davies (1971) and Kwan & Ko (1976), most of the energy of the spectra is under the broad peak. Hence a comparison of the overall pressure intensity of the ellipsoidal and conical annular jets with that of the single jet would be almost equivalent to a comparison of the energy under the broad peak. In this way, the extremely good agreement of the overall pressure intensity of the two annular jets with that of the single jet confirms that the characteristics of the jet vortices in the mixing regions of these types of jet are the same.

The spectra of the pressure fluctuations of the basic annular jet, however, give a slightly different picture (figure 11). The spectra at the axis of the potential core,

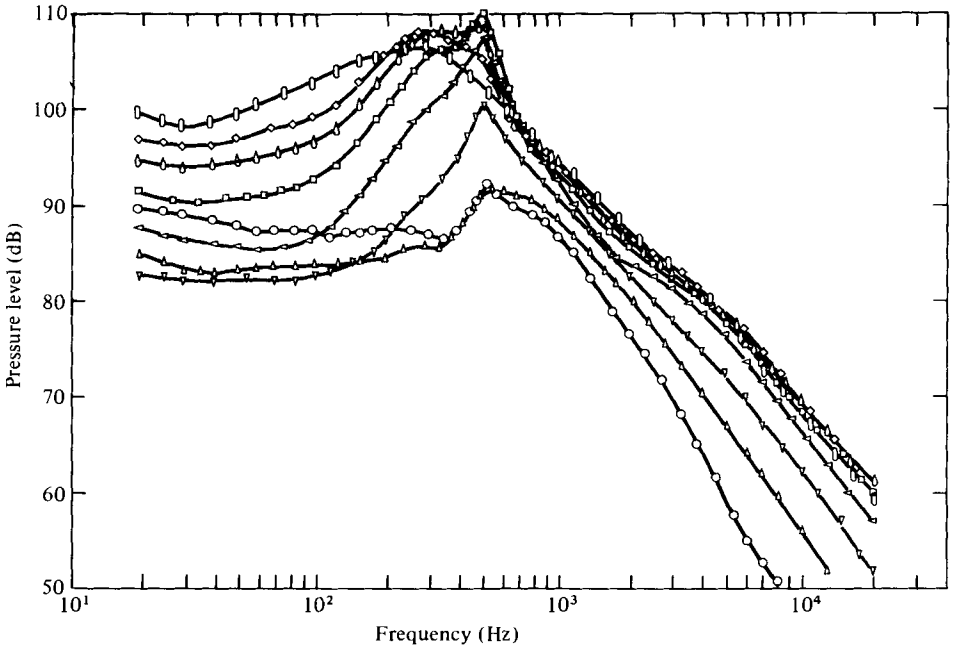

FIGURE 11. Spectra of microphone signals for basic annular jet ($y/D_0 = 0{\cdot}3$). x/D_0: ○, 0·5; △, 0·75; ▽, 1; ◁, 1·5; □, 2; ⬯, 2·5; ◇, 3; ▽, 3·5; ⬯, 4.

$y/D_o = 0{\cdot}3$, show the presence of the jet vortices. However, the broad peak in the initial merging zone ($x/D_o \leqslant 1{\cdot}5$), due to the jet vortices, is not as obvious as the one in the intermediate merging zone. This is due to the interference of the sharp peak present in the spectra, which, as will be discussed in detail elsewhere, is due to the wake vortices. The peak frequency of the wake vortices, as shown in figure 11, is nearly constant at 530 Hz over the axial distance considered. This constancy of the peak frequency of the wake vortices does not hold for the jet vortices. The peak frequency of the latter, as will also been shown in the section on the Strouhal number (§ 7), is lower further downstream (figure 10). The difference between the peak frequencies of these two types of vortex may also be the reason for the different appearance of the broad peak in the intermediate merging zone (figure 11). It is also within the intermediate zone that the sharp peak starts to disappear from the spectra. After reaching a maximum amplitude at $2 \leqslant x/D_o \leqslant 2{\cdot}5$, the peak disappears at $x/D_o = 4$. This further indicates the region in which the wake vortices are present and their effect felt.

The pressure fluctuations of both the jet and the wake vortices within the potential core of the annular jet are also sensed at the central axis $y/D_o = 0$ (figure 12). The sharp peak due to the wake vortices is also found around 530 Hz and has both the same frequency and almost the same shape as the one observed inside the potential core (figure 11). Instead of having a maximum amplitude at $2 \leqslant x/D_o \leqslant 2{\cdot}5$, the maximum of the wake vortices at the central axis occurs at $x/D_o = 0{\cdot}5$. This position is the estimated point to which the recirculating flow extends. In other words, the maximum amplitude is found within the recirculating region, where the wake vortices are generated.

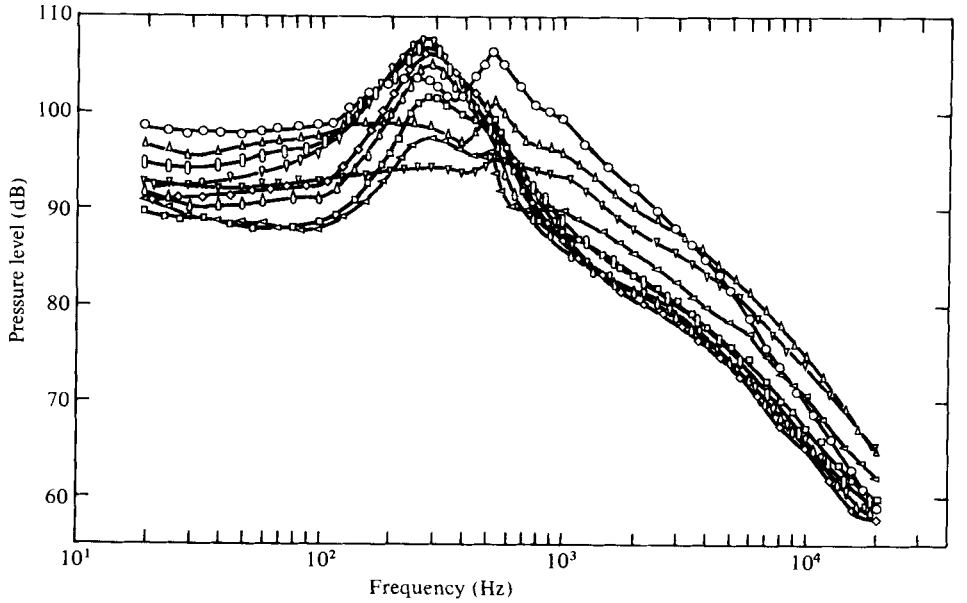

FIGURE 12. Spectra of microphone signals along central axis of basic annular jet ($y/D_0 = 0$). Symbols same as in figure 11.

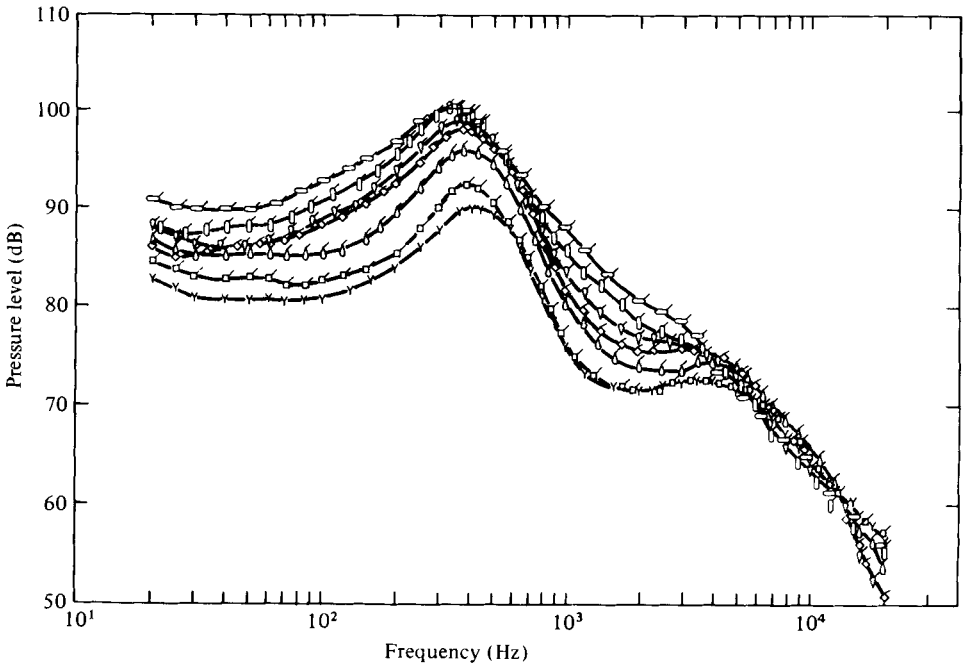

FIGURE 13. Spectra of microphone signals along central axis of ellipsoidal jet ($y/D_0 = 0$). Symbols same as in figure 9.

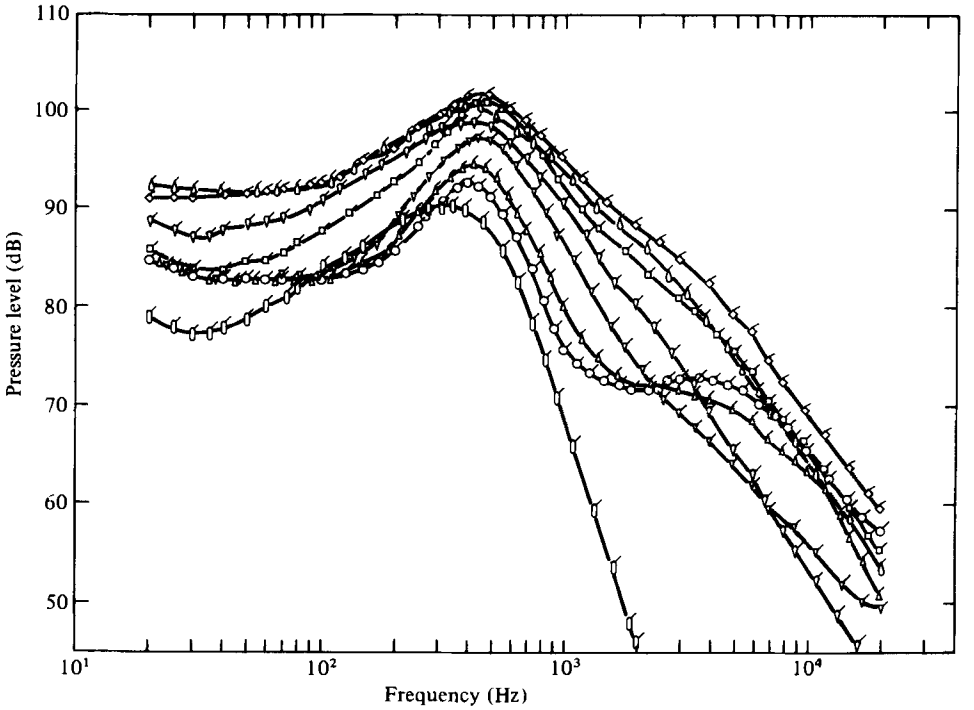

FIGURE 14. Spectra of microphone signals at different radial positions in ellipsoidal jet ($x/D_0 = 2$). y/D_0: ○, 0; △, 0·1; ▽, 0·2; □, 0·3; ◇, 0·4; ⬡, 0·5; ⬡, 0·6; ⬡, 0·8.

At the central axis $y/D_o = 0$ the jet vortices of the basic annular jet have a maximum amplitude at $x/D_o = 3{\cdot}5$. This position is similar to the one obtain at $y/D_o = 0{\cdot}3$ but the peak frequency is different, having a nearly constant value of 260 Hz in the intermediate merging zone $1{\cdot}5 \leqslant x/D_o \leqslant 4$. In the initial merging zone $x/D_o \leqslant 1$, however, the peak seems to be slightly different from that observed in the intermediate merging zone. The peak amplitude has a high value at $x/D_o = 0{\cdot}5$ then decreases till $x/D_o = 1$ before increasing again. It is not certain what factors cause this behaviour of the broad peak in the recirculating region of the basic annular jet, especially at $x/D_o = 0{\cdot}5$. It may be due to the standing vortex, yet to be shed downstream, in the recirculating region. This means that the sharp peak at 530 Hz may be due to the wake vortices which are shed downstream while the one at 260 Hz at $x/D_o = 0{\cdot}5$ may be due to the standing vortex.

This broad peak of 260 Hz at $x/D_o = 0{\cdot}5$ cannot be due to the jet vortices found in the outer mixing region. As can be seen from the spectra in the potential core (figure 11), the peak pressure amplitude of the jet vortices for $x/D_o \leqslant 0{\cdot}75$ is about 90 dB and is observed at a higher frequency, about 700–800 Hz. Thus the amplitude is far lower than the amplitude observed at the central axis. At the central axis, a peak pressure level of 103 dB is found at $x/D_o = 0{\cdot}5$ and one of 99 dB at $x/D_o = 0{\cdot}75$. Rather, detailed inspection of figure 11 shows the trace of a spectral peak at $x/D_o = 0{\cdot}5$ and 0·75 of between 200 and 300 Hz. The pressure amplitude of the peak at $x/D_o = 0{\cdot}5$ is 86 dB while that at $x/D_o = 0{\cdot}75$ is 83 dB. Although their amplitude is lower by about 16 dB, these peaks are very similar to the ones observed at the central axis

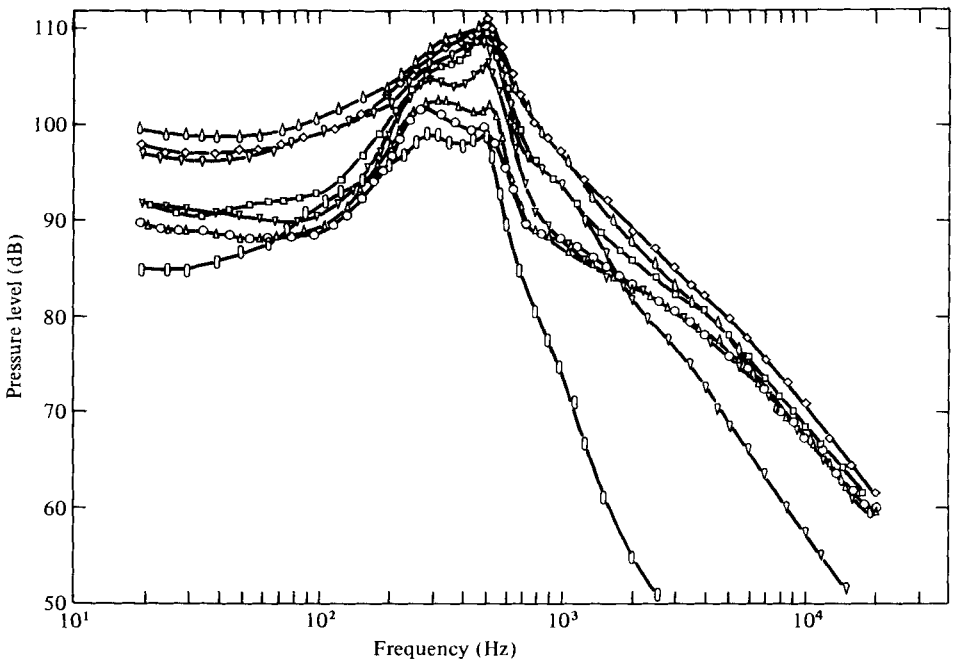

FIGURE 15. Spectra of microphone signals at different radial positions in basic annular jet ($x/D_0 = 2$). y/D_0: ○, 0; △, 0·1; ▽, 0·2; □, 0·3; ◇, 0·4; ⬯, 0·5; ⬯, 0·6; ⬯, 0·8.

(figure 12). In this respect, the above observation strongly suggests that the broad peak at $0{\cdot}5 \leqslant x/D_0 \leqslant 0{\cdot}75$ is generated in or near the recirculating region. Because of its low energy, its effect outside its source region is detected only in a low intensity region such as the potential core.

These wake vortices observed in the basic annular jet are absent when the recirculating region is removed. Thus the spectra at the central axis of the ellipsoidal (figure 13) and conical jets do not have these peaks, except the one due to the jet vortices. At the central axis the peaks of both the ellipsoidal and the conical jet saturate at the axial position $4 \leqslant x/D_0 \leqslant 4{\cdot}5$.

In addition, a peak at the higher frequency 4000 Hz and lower pressure level 72 dB is found at the axis (figure 13). It is observed only within the axial region $1{\cdot}75 \leqslant x/D_0 \leqslant 3{\cdot}5$ with a maximum at $x/D_0 = 2{\cdot}5$ and may be due to the tiny wake formed behind the bullet.

Radial distributions of the pressure spectra at the axial position $x/D_0 = 2$ are shown in figures 14 and 15. As would be expected, the spectra of the ellipsoidal jet are mainly due to the contribution from the jet vortices (figure 14). The effect of the jet vortices is felt across the whole radial range considered, from the central axis ($y/D_0 = 0$) to the boundary with the entrainment region ($y/D_0 = 0{\cdot}8$). The maximum of the peak and also of the energy under the peak in the spectrum is found at $y/D_0 = 0{\cdot}4$. This radial position agrees very well with the one observed in the overall pressure measurements (figure 6). This agreement further confirms that the overall pressure intensity is mainly due to the energy under the peak in the spectrum.

Agreement of the position is difficult to find for the basic annular jet (figure 15). The reason is the presence of two peaks: the sharp one due to the wake vortices and the

	Annular jet		
	Initial merging zone, outer mixing region	Intermediate zone	Single jet
Strouhal number, St_*	$f_j D_0/\overline{U}_0$	$f_j D_0/\overline{U}_m$	$f_j D/\overline{U}_0$

TABLE 1. Definition of Strouhal number of annular jets.

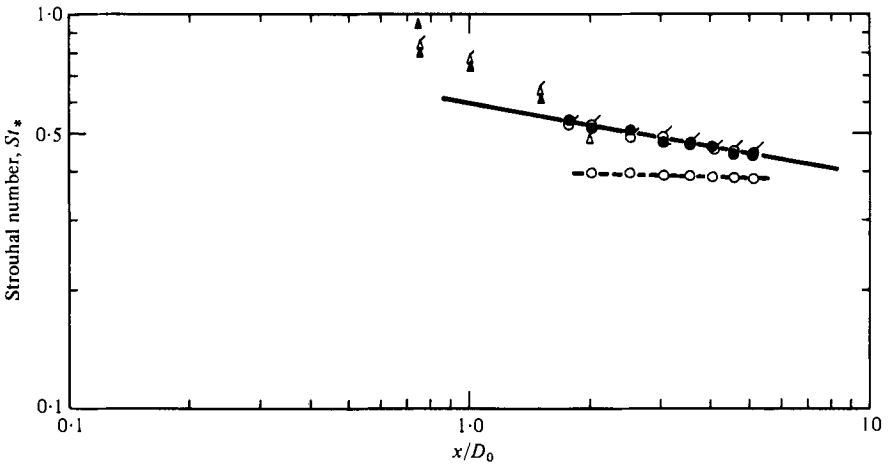

FIGURE 16. Axial distributions of Strouhal number of jet vortices in intermediate merging zone. $y/D_0 = 0$: ○, annular jet; ●, conical jet; ♂, ellipsoidal jet; ——, single jet (Ko & Davies 1971). $y/D_o = 0{\cdot}3$; ▲, conical jet; ⍙, ellipsoidal jet.

broad one due to the jet vortices. Furthermore, because their frequencies are fairly close together and their amplitudes are roughly the same, the energy under these peaks is about the same. This means that their contributions to the overall pressure intensity render the interpretation of the overall measurements unreliable. This may also be the reason why the maximum amplitude of the wake vortex appears at $0{\cdot}4 \leqslant y/D_o \leqslant 0{\cdot}5$.

7. Strouhal number

As has been discussed above, the flow structures of the ellipsoidal and conical jets are more easily understood as the bullet eliminates complications due to wake vortices inside the jets. Thus the broad peak observed in the spectral measurements is identical to that for a single jet, i.e. is due to the jet vortices found in the mixing region. Besides the similarity of the peak, the pressure intensities of the jet vortices in the outer mixing region of these two annular jets have the same characteristics as that for a single jet (figure 8). The above agreement suggests beyond doubt that the broad peak in the spectral measurements is due to the jet vortices.

The present section compares the Strouhal numbers corresponding to the peak frequency f_j of the jet vortices in the outer mixing region of the ellipsoidal and conical

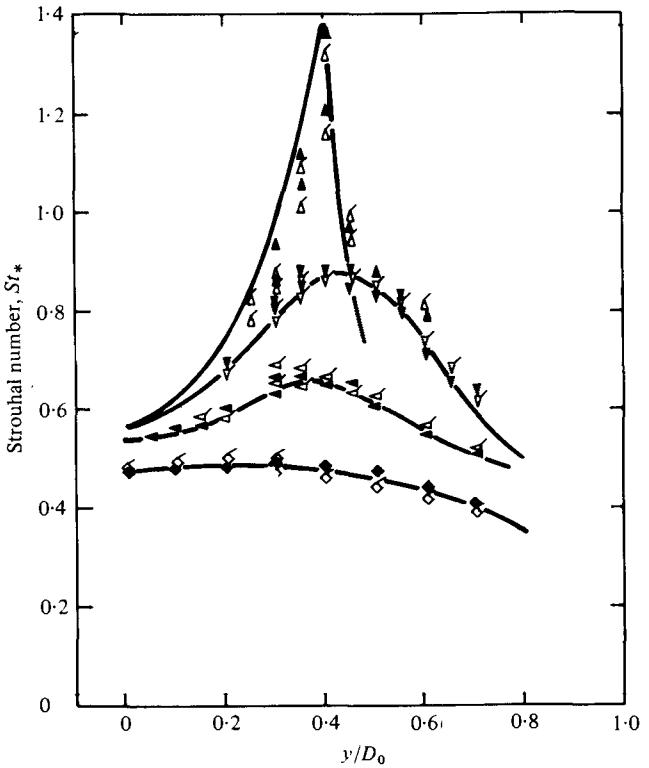

FIGURE 17. Radial distributions of Strouhal number of jet vortices. Conical jet, x/D_0: ▲, 0·75; ▼, 1; ◀, 1·5; ◆, 3. Ellipsoidal jet, x/D_0: △, 0·75; ▽, 1; ◁, 1·5; ◇, 3. ——, single jet (Ko & Davies 1971).

jets with that of a single jet. The Strouhal numbers in the initial and intermediate merging zones are defined in table 1.

The axial distributions of the Strouhal number of the annular jets are shown in figure 16. The distribution within the initial merging zone is for $y/D_o = 0{\cdot}3$, i.e. near the axis of the potential core. Within the intermediate merging zone the distribution is along the central axis $y/D_o = 0$. It is interesting to find that in the intermediate merging zone the Strouhal numbers of the peak frequency of the jet vortices at the central axis $y/D_o = 0$ of the ellipsoidal and conical jets agree very well with those of the single jet. In the initial merging zone, because of the presence of the bullet comparison is made of the Strouhal numbers near the axis of the potential core ($y/D_o = 0{\cdot}3$). The Strouhal numbers of the two annular jets are higher than those of the single jet.

The radial distributions of the Strouhal number of the ellipsoidal and conical jets are shown in figure 17. The single-jet results of Ko & Davies (1971) are included for comparison. Except for a slight deviation of the values at $x/D_o = 0{\cdot}75$, the Strouhal numbers of the two annular jets agree very well with those of the single jet. It is further found that a peak of the Strouhal number distributions is also observed for the two annular jets.

8. Discussion

In the initial merging zone, perhaps because of the shrouding effect of the annular potential core, the outer mixing region is less strongly affected by the inner mixing region. Therefore the outer mixing regions of all three annular jets give the same flow characteristics as that observed in a single jet.

In the intermediate merging zone of the ellipsoidal and conical jets, owing to the elimination of the recirculating region, the overall pressure measurements and spectral properties agree very well with those of a single jet. In the case of the basic annular jet, the overall pressure measurements are correspondingly higher inside the boundary of the jet. The growth of the jet vortices seems to saturate in $2 \leqslant x/D_o \leqslant 3{\cdot}5$, and extends further upstream than for the other two annular jets and the single jet.

Within the axial distance considered, $0{\cdot}5 \leqslant x/D_o \leqslant 5$, the Strouhal number of the three annular jets corresponds to that of the single jet. This agreement extends to the fully developed region of the single jet, $x/D = 8$. This agreement further supports the finding from the mean velocity that all three annular jets are fully developed at around $x/D_o = 5$. Therefore the presence of the central recirculating region and the wake vortices in the basic annular jet have the effect of accelerating the jet into the fully developed state. This explains the deviation of the flow characteristics in the intermediate merging zones of the annular three jets from those of a single jet.

The good correlation of the results for the annular jets pertaining to the outer mixing region with those for the single jet, especially in the initial merging zone, can be explained by the similarity of the flow structure in the mixing regions of the two types of jet. Thus the outer mixing region can be thought of as the result of the shearing of a single jet of diameter D_o and mean exit velocity $\overline{U}_0$ by the ambient air. Therefore it is reasonable to suggest the existence of an array of toroidal vortices convecting downstream in the outer mixing region.

Very good agreement with the above results is obtained with the jet running at an exit velocity of 30 m/s. In particular, the spectral properties are found to be similar within the velocity range 10–60 m/s.

The work was supported in part by a research grant from the University of Hong Kong.

REFERENCES

ABRAMOVICH, N. 1963 *The Theory of Turbulent Jets*. M.I.T. Press.

BEER, J. M. & CHIGIER, N. A. 1972 *Combustion Aerodynamics*. Applied Science Publishers.

BRADSHAW, P., FERRISS, D. H. & JOHNSON, H. F. 1964 Turbulence in the noise-producing region of a circular jet. *J. Fluid Mech.* **19**, 591–624.

CARMODY, T. 1964 Establishment of the wake behind a disk. *Trans. A.S.M.E., J. Basic Engng* D **86**, 869–882.

CHAN, W. T. 1977 Flow structures of annular jets. M.Ph. thesis, University of Hong Kong.

CHIGIER, N. A. & BEER, J. M. 1964 The flow region near the nozzle in double concentric jets. *Trans. A.S.M.E., J. Basic Engng* D **86**, 797–804.

CROW, S. C. & CHAMPAGNE, G. H. 1971 Orderly structure in jet turbulence. *J. Fluid Mech.* **48**, 547–591.

DAVIES, P. O. A. L., FISHER, M. J. & BARRATT, M. J. 1963 The characteristics of the turbulence in the mixing region of a round jet. *J. Fluid Mech.* **15**, 337–367.

DAVIES, T. W. & BEER, J. M. 1969 The turbulence characteristics of annular wake flow. *Heat Mass Transfer in Flows with Separated Regions, Int. Sem., Hercig-Novi, Yugoslavia,*

FISHER, M. J. & DAVIES, P. O. A. L. 1964 Correlation measurements in a non-frozen pattern of turbulence. *J. Fluid Mech.* **18**, 97–116.

FUCHS, H. V. 1972 Measurements of pressure fluctuations within subsonic turbulent jets. *J. Sound Vib.* **22**, 361–378.

KO, N. W. M. & CHAN, W. T. 1978 Similarity in the initial region of annular jets: three configurations. *J. Fluid Mech.* **84**, 641–656.

KO, N. W. M. & DAVIES, P. O. A. L. 1971 The near field within the potential core of subsonic cold jets. *J. Fluid Mech,* **50**, 49–78.

KO, N. W. M. & DAVIES, P. O. A. L. 1975 Some covariance measurements in a subsonic jets. *J. Sound Vib.* **41**, 347–358.

KO, N. W. M. & KWAN, A. S. H. 1976 The initial region of subsonic coaxial jets. *J. Fluid Mech.* **73**, 305–332.

KWAN, A. S. H. & KO, N. W. M. 1976 Coherent structures in subsonic coaxial jets. *J. Sound Vib.* **48**, 203–219.

KWAN, A. S. H. & KO, N. W. M. 1977 Covariance measurement in the initial region of coaxial jet. *J. Sound Vib.* **52**, 567–578.

LAU, J. C. 1971 The coherent structure of jets. Ph.D. thesis, University of Southampton.

LAU, J. C., FISHER, M. J. & FUCHS, H. V. 1972 The intrinsic structure of turbulent jets. *J. Sound Vib.* **22**, 379–406.

MILLER, D. R. & COMINGS, E. W. 1960 Force-momentum fields in a dual-jet flow. *J. Fluid Mech.* **7**, 247–256.

VANDERBURY, W. H. 1973 Applications of dual jet flows to fluidics. Ph.D. thesis, University of Waterloo.

WILLIAMS, T. J., ALI, M. R. M. H. & ANDERSON, J. S. 1969 Noise and flow characteristics of coaxial jets. *J. Mech. Engng Sci.* **11**, 133–142.